Mon. Not. R. Astron. Soc. **000**, 000–000 (0000) Printed 3 April 2014 (MN LATEX style file v2.2)

Binarity in Carbon-Enhanced Metal-Poor stars⋆

Else Starkenburg[1]†‡, Matthew D. Shetrone[2], Alan W. McConnachie[3] and Kim A. Venn[1]
[1] *Dept. of Physics and Astronomy, University of Victoria, P.O. Box 3055, STN CSC, Victoria BC V8W 3P6, Canada*
[2] *McDonald Observatory, The University of Texas at Austin, 1 University Station, C1400, Austin, TX 78712-0259, USA*
[3] *NRC Herzberg Institute of Astrophysics, 5071 West Saanich Road, Victoria, BC, V9E 2E7, Canada*

arXiv:1404.0385v1 [astro-ph.SR] 1 Apr 2014

3 April 2014

ABSTRACT
A substantial fraction of the lowest metallicity stars show very high enhancements in carbon. It is debated whether these enhancements reflect the stars' birth composition, or if their atmospheres were subsequently polluted, most likely by accretion from an AGB binary companion. Here we investigate and compare the binary properties of three carbon-enhanced sub-classes: The metal-poor CEMP-s stars that are additionally enhanced in barium; the higher metallicity (sg)CH- and Ba II stars also enhanced in barium; and the metal-poor CEMP-no stars, not enhanced in barium. Through comparison with simulations, we demonstrate that all barium-enhanced populations are best represented by a $\sim$100% binary fraction with a shorter period distribution of at maximum $\sim$20,000 days. This result greatly strengthens the hypothesis that a similar binary mass transfer origin is responsible for their chemical patterns. For the CEMP-no group we present new radial velocity data from the Hobby-Eberly Telescope for 15 stars to supplement the scarce literature data. Two of these stars show indisputable signatures of binarity. The complete CEMP-no dataset is clearly inconsistent with the binary properties of the CEMP-s class, thereby strongly indicating a different physical origin of their carbon enhancements. The CEMP-no binary fraction is still poorly constrained, but the population resembles more the binary properties in the Solar Neighbourhood.

Key words: stars: chemically peculiar – galaxies: formation – Galaxy: halo – stars: abundances – stars: AGB and post-AGB – stars: binaries

1 INTRODUCTION

The lowest metallicity stars that still exist today probably carry the imprint of very few supernovae. As such, they represent our best observational approach to understanding of the First Stars. The number of metal-poor stars in the Galactic halo with abundance determinations has bloomed recently; now over 150 stars with [Fe/H] < -3 have been examined in high-resolution studies (see for some recent overviews and results: Aoki et al. 2013; Yong et al. 2013a; Cohen et al. 2013; Spite et al. 2013; Placco et al. 2014). In addition to stars with a normal chemical composition (those continuing the well-defined trends of elemental abundances at higher metallicities), various chemically peculiar stars are found. The intriguing question therefore is if these chemical anomalies tell us something about the very first stages of star formation?

Probably the most significant chemical sub-group is that of carbon-enhanced metal-poor (CEMP) stars. The fraction of extremely metal-poor stars which are carbon-enhanced is as high as 32-39% for stars with [Fe/H]<-3 (Yong et al. 2013b; Aoki et al. 2013; Lee et al. 2013), which then decreases to 9-21% for [Fe/H]<-2.0 (e.g., Norris, Ryan & Beers 1997a; Rossi, Beers & Sneden 1999; Christlieb 2003; Marsteller et al. 2005; Lucatello et al. 2006; Cohen et al. 2005; Frebel et al. 2006; Carollo et al. 2012; Lee et al. 2013)[1]. The fraction of CEMP stars is not just dependent on the metallicity, but also seems to vary with the distance above the Galactic plane (Frebel et al. 2006; Carollo et al. 2012) and between the inner and outer halo component (Carollo et al. 2012, 2014). Measurements of [C/Fe] for extremely metal-poor stars range all the way up to [C/Fe]$\sim +4.0$.

A substantial fraction of CEMP stars also show an overabundance in heavy elements, these are generally called "CEMP-s", "CEMP-r", or "CEMP-r/s" depending on the exact abundance and ratio of s-process and r-process elements. Beers & Christlieb (2005) have developed the following nomenclature that we will fol-

⋆ Based on observations obtained with the Hobby-Eberly Telescope, which is a joint project of the University of Texas at Austin, the Pennsylvania State University, Stanford University, Ludwig-Maximilians-Universität München, and Georg-August-Universität Göttingen.
† email: else@uvic.ca
‡ CIFAR Global Scholar

[1] We caution that various definitions of carbon-enrichment are used between different authors. Generally, a limit of [C/Fe]=+1.0 or [C/Fe]=+0.7 is used, although some authors prefer a limit that is dependent on the luminosity of the star to take into account internal mixing of carbon on the red giant branch (e.g. Aoki et al. 2007).

© 0000 RAS

low in this paper (note that the different classes as defined here are not necessarily mutually exclusive):

- CEMP-r: [C/Fe] $>$ +1.0 and [Eu/Fe] $>$ +1.0
- CEMP-s: [C/Fe] $>$ +1.0, [Ba/Fe] $>$ +1.0, and [Ba/Eu] $>$ +0.5
- CEMP-r/s: [C/Fe] $>$ +1.0 and 0.0 $<$ [Ba/Eu] $<$ +0.5
- CEMP-no: [C/Fe] $>$ +1.0 and [Ba/Fe] $<$ 0

The large class of CEMP-s stars are thought to obtain their overabundant carbon and s-process elements from a companion star that has gone through the AGB phase and deposited large amounts of newly formed carbon and s-process material on its neighbour. Strong evidence in favour of this scenario was found from repeated radial velocity measurements. The fraction of stars that show significant velocity variability in the CEMP-s class is sufficiently high to comfortably support the claim that all such stars might indeed be in binary systems (Lucatello et al. 2005, and references therein).

Based on their abundance patterns, it has been suggested that the CEMP-r/s class has the same binary origin as the CEMP-s stars (e.g., Masseron et al. 2010; Allen et al. 2012), although this might mean that a different neutron-capture process with features in between the r- and s-process will need to be invoked (Lugaro et al. 2012, Herwig et al., in preparation) to provide for its particular chemical signatures. An alternative explanation is that CEMP-r/s stars originate in regions already enriched in r-process elements and are subsequently enriched in s-rich material by a companion (e.g., Bisterzo et al. 2012).

CEMP-r stars are very rare, but Hansen et al. (2011) studied one CEMP-r star in their careful radial velocity monitoring program of r-process-enhanced stars. This star, CS 22892–052, shows no sign of binarity.

The origin of the CEMP-no class is debated (e.g. Ryan et al. 2005; Masseron et al. 2010; Norris et al. 2013b). The absence of the signature s-process overabundance, which is thought to be produced in AGB stars just as the overabundant carbon, gives reason to believe these stars might not obtain their peculiar abundance pattern due to mass transfer in binary systems. Under the premise that CEMP-no stars are *not* in binary systems, another explanation has to be offered for the overabundance of carbon and other light elements in these stars. One proposed origin for their chemical pattern is that these stars are truly second generation stars and formed from gas clouds already imprinted with a large overabundance of carbon and other light elements by the First Stars (e.g. Bromm & Loeb 2003; Norris et al. 2013b; Gilmore et al. 2013). The fact that almost all of the stars with [Fe/H]$\leq$-4.0 are of the CEMP-no class seems to favor such an explanation. In particular, four out of the five stars known with [Fe/H]$<$-4.5 seem to be consistent with the CEMP-no class (Christlieb et al. 2004; Frebel et al. 2005; Aoki et al. 2006; Norris et al. 2007; Keller et al. 2014, although in some cases only an upper limit for barium could be derived). Note also the exception from Caffau et al. (2011).

On the other hand, it is yet insufficiently understood if carbon could be transferred from an AGB companion without s-process elements (e.g., Suda et al. 2004). Mass-transfer mechanisms that would transfer carbon – but no or few s-process elements – are theoretically expected from massive AGB stars with hot dredge-up, terminating the AGB process before the star had time to develop s-process elements (Herwig 2004), or some rotating AGB companions (Herwig, Langer & Lugaro 2003; Siess, Goriely & Langer 2004). However, this result is dependent on the parameters adopted, as shown by Piersanti, Cristallo & Straniero (2013). Komiya et al. (2007) argue that relative high-mass AGB stars could be the companions of CEMP-no stars as they produce less s-process elements. But a problem with this scenario is that these stars would produce a lot of nitrogen, a signature that not all CEMP-no stars share (see for instance Ito et al. 2013; Norris et al. 2013b). It has also been suggested that in very low-metallicity AGB-stars with very high neutron-to-Fe-peak-element seed ratios, the s-process runs to completion and a large overabundance of Pb is produced instead of Ba (Busso, Gallino & Wasserburg 1999; Cohen et al. 2006). Because Pb absorption lines are very weak and the strongest line in the optical overlaps with the CH-feature, this hypothesis is difficult to test, especially in C-rich stars. A robust upper limit could nonetheless be given for the brightest CEMP-no star, BD +44-493, which did not show the predicted overabundance in Pb (Ito et al. 2013).

In analogy with the work on CEMP-s stars by Lucatello et al. (2005) and others, we might be able to settle this debate using radial velocity monitoring. If CEMP-no stars are also products of binary evolution, this would show itself in radial velocity variations of the stars. From such an exercise, Norris et al. (2013b) conclude that there is little support for a binary origin for CEMP-no stars, unlike with the CEMP-s stars. But, as an overview of the available literature data such as presented in Table 5 of Norris et al. (2013b) makes clear, there is a lack of systematic radial velocity studies with sufficient accuracy and cadence to carry out a conclusive quantitative study. For 43% of the stars there is only one radial velocity measurement available, making it impossible to tell whether they are part of a binary system. Most other stars have less than 5 measurements published in the literature. The two stars that have been most thoroughly researched, BD +44-493 and CS 22957-027, do show evidence for velocity variations, but these variations are comparable to the observational uncertainties in the case of BD +44-493. Radial velocity data for eight more stars has in the meantime been added (Hansen, Andersen & Nordtröm 2013, also Andersen et al., in preparation). They find that two out of their sample of eight CEMP-no stars are in binary systems. Due to these small numbers, it is not at all clear if CEMP-no stars have binary companions, and the presence of a companion may well influence their evolution.

This current scarcity of data severely limits our understanding of the very first epochs of star formation. In this work, we present additional radial velocity measurements for 15 CEMP-no stars. Additionally, we homogeneously analyze and model the binary fraction and period distribution of binaries in the CEMP-no class, the CEMP-s class and the – much more metal-rich – CH-, sgCH- and Ba II-stars. Based on the comparative binary properties of each of these classes, we then go on to discuss their nature.

In Section 2 we present the new data from this work. In Section 3 we use these data for the CEMP-no stars to analyze velocity variations and constrain their binary properties. Section 4 is devoted to comparison with simulations for the CEMP-no, CEMP-s and CH-, sgCH- and Ba II-stars. This analysis leads to various conclusions and hypotheses for the nature of these stars, as discussed in Section 5.

2 DATA

Radial velocity measurements were obtained using the High Resolution Spectrograph (HRS, Tull 1998) with resolving power R=18000 on the Hobby-Eberly Telescope (HET, Ramsey et al. 1998) from January to August 2013, as part of normal queue observing (Shetrone et al. 2007), after which the HET was taken offline for installation of new instrumentation. During this period, all extremely metal-poor CEMP-no stars as compiled by Norris et al. (2013b) in reach of HET were targeted at least twice. This sample

Star	Vmag	T_{eff} (K)	logg	[Fe/H]	[C/Fe]	[Ba/Fe]	# Vr lit. meas.	Source	$p(\chi^2\|f)$ lit. 1σ	$p(\chi^2\|f)$ this work 1σ	$p(\chi^2\|f)$ both 1σ	$p(\chi^2\|f)$ both 3σ
53327-2044-515_d	15.1	5703	4.68	−4.00	+1.13	$<$ +0.34	3	1, 13	0.62	0.11	0.00	0.53
53327-2044-515_g	15.1	5703	3.36	−4.09	+1.57	$<$ −0.04	3	1, 13	–	–	–	–
BD +44-493	9.1	5510	3.70	−3.68	+1.31	−0.59	28	2, 14	0.02	0.92	0.00	1.00
BS 16929-005	13.6	5229	2.61	−3.34	+0.99	−0.41	3	1, 7, 8	0.06	0.82	0.00	0.74
CS 22878-027	14.8	6319	4.41	−2.51	+0.86	$<$ −0.75	2	1, 8	0.00	0.58	0.04	0.98
CS 22949-037	14.4	4958	1.84	−3.97	+1.06	−0.52	10	1, 4, 9-11, 16-19	0.21	0.72	0.32	1.00
CS 22957-027	13.6	5170	2.45	−3.19	+2.27	−0.80	15	1, 5, 12, 20, 23	0.00	0.95	0.00	0.00
CS 29502-092	11.9	5074	2.21	−2.99	+0.96	−1.20	3	1, 8	0.00	0.92	0.00	0.19
HE 1150−0428	14.9	5208	2.54	−3.47	+2.37	−0.48	2	1, 5, 23	0.00	0.00	0.00	0.00
HE 1300+0157	14.1	5529	3.25	−3.75	+1.31	$<$ −0.85	4	1, 4, 6, 15	0.65	0.50	0.72	1.00
HE 1506−0113	14.8	5016	2.01	−3.54	+1.47	−0.80	4	1, 13	0.30	0.00	0.00	0.00
Segue 1-7	17.7	4960	1.90	−3.52	+2.30	$<$ −0.96	1	3	–	0.83	0.58	0.97
SDSS J1422+0031	16.3	5200	2.2	−3.03	+1.70	−1.18	2	21, 22	0.01	–	0.00	0.01
SDSS J1613+5309	16.4	5350	2.1	−3.33	+2.09	+0.03	2	21, 22	0.40	0.46	0.74	0.99
SDSS J1746+2455	15.7	5350	2.6	−3.17	+1.24	+0.24	2	21, 22	0.97	0.58	0.43	0.98
SDSS J2206-0925	14.9	5100	2.1	−3.17	+0.64	−0.85	2	21, 22	0.49	–	0.63	0.95

Table 1. Overview of literature data and derived probabilities for binarity for the targeted sample of CEMP-no stars in this work. Shown here are the literature values for the V-magnitude of the stars, derived Teff and log(g) (two possible solutions are given for 53327-2044-515), [Fe/H], [C/Fe] and [Ba/Fe]. The subsequent number of radial velocity literature measurements deviates slightly from the similar compilation of Norris et al. (2013b) for a few stars. These differences arise because we count all individual measurements (also if they are on the same or adjecent days) as long as the velocities per observation are given separately in the relevant literature. The last four columns show the derived probabilities that the observed scatter in velocities is due to measurement errors (see text for details) for the data in the literature and this work both separately and combined. The last column shows the probability for the combined dataset, but inflating σ_{vr_i} by a factor of 3. References: 1 = Yong et al. (2013a); 2 = Ito et al. (2009), 3 = Norris et al. (2010), 4 = Cohen et al. (2008), 5 = Cohen et al. (2006), 6 = Frebel et al. (2007a), 7 = Honda et al. (2004), 8 = Lai et al. (2008), 9 = Cayrel et al. (2004), 10 = Spite et al. (2005), 11 = François et al. (2007), 12 = Norris, Ryan & Beers (1997b), 13 = Norris et al. (2013a), 14 = Carney et al. (2003), 15 = Barklem et al. (2005), 16 = McWilliam et al. (1995a), 17 = McWilliam et al. (1995b), 18 = Norris, Ryan & Beers (2001), 19 = Depagne et al. (2002),20 = Preston & Sneden (2001), 21 = Aoki et al. (2013), 22 = SDSS SSPP DR9, 23 = Cohen et al. (2013)

is restricted to CEMP-no stars that additionally have [Fe/H]<–3.0, with one exception (CS 22878-027). We note that 53327-2044-515 will have an upper limit of [Ba/Fe] $<$ +0.34 if the star is on the main-sequence and thus might or might not qualify the restrictions for CEMP-no stars. In addition to this sample, we targeted four new extremely metal-poor targets with CEMP-no-like abundance patterns, as published in Aoki et al. (2013). Although here we also note that two of these targets stars are on the border of the CEMP-no star definition, because of their [Ba/Fe] determination that is slightly above the solar ratio (although clearly not enhanced to the [Ba/Fe]=+1 level of CEMP-s stars). J2206-0925 has [C/Fe] = +0.64, which is slightly lower than the often used limit of +0.70 for carbon-rich stars. An overview of the literature stellar parameters and abundance ratios for these targets is presented in Table 1.

For our targets, we calculated exposure times to obtain a minimum S/N of ∼20. Directly after each target a Th-Ar exposure was taken and on nearly every night (weather permitting) a radial velocity standard was observed during twilight. Radial velocities were computed by means of cross-correlating a synthesized extremely metal-poor carbon-enhanced spectrum with the observed spectrum and standard, using the velocity of the standard as calibration for the zero point. The choice of a zero-point based on radial velocity standards is strengthened by a clear observed trend of the radial velocity standards' offsets with their literature values versus the observation date. The total magnitude of this variation over the full observing period is 2.7 km s^{-1} with small scatter. We are uncertain about its origin. However, since our radial velocity standards are observed at a similar time and comparable air-mass to our targets, any systematic effects that could be the cause of this offset in telescope, instrument or analysis are not propagated in our results.

To obtain the 1-σ error bars on the measurements presented in this paper we added in quadrature the individual 1-σ errors in the radial velocity cross-correlations with each spectrum and a subsequent error floor of 0.26 km s^{-1}. This error floor is based on the rms variations in all standard stars once corrected for the aforementioned variation with the date of the observation by a simple 4th order polynomial fit. The final heliocentric velocities and their errors for our observations are presented in Table 2.

3 RESULTS

3.1 Radial velocity variations

In Figure 1 we show the maximum velocity variation between two measurements for all stars observed in this program, taking into account the data obtained in this work and literature data both separately and combined. Two stars very clearly stand out: both HE 1150-0428 and HE 1506-0113 are varying by more than 10 km s^{-1} over the 74 and 132 days these stars were observed with the HET. Moreover, the currently observed heliocentric velocity of HE 1506-0113 differs by over 57 km s^{-1} from the measured velocity by Norris et al. (2013a).

In addition to binarity, flows, pulsations and inhomogeneities on the stellar surface can also present themselves in observed radial velocity variations. Considering the precision of this study, this so-called radial velocity "jitter" – although theoretically poorly understood – is expected to (only) manifest itself clearly at the tip of the red giant branch (e.g. Gunn & Griffin 1979; Setiawan et al. 2003; Wright 2005; Carney et al. 2008). Carney et al. (2008) find

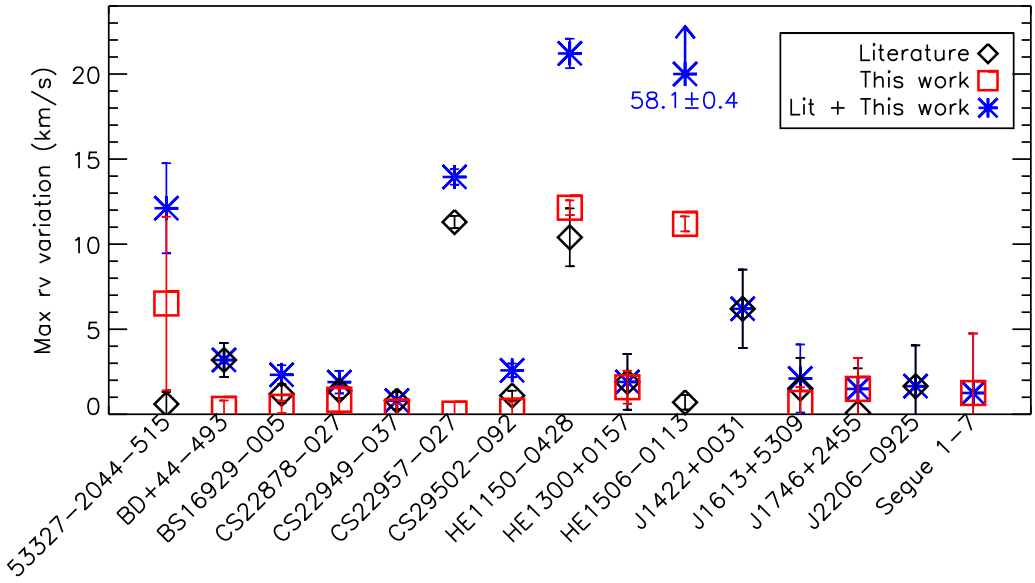

Figure 1. Maximum velocity variation for each of the stars observed in this work. The largest difference between two measurements is shown for the data presented in Table 2 (red squares), literature data only (black diamonds) and both datasets combined (blue asterisks). If one of the subsets had only one measurement, the plotting symbol for that subset is omitted. Error bars reflect the measurement errors on both measurements involved. The velocity difference between our data and the literature measurement for HE 1506-0113 is beyond the scale of this figure, its value is shown in the panel instead.

in their monitoring program of metal-poor stars that jitter is present in most stars with $M_V < -2.0$ and in a significant number of stars with $M_V < -1.4$. Based on their results, they cannot exclude that velocity jitter is not contributing at lower magnitudes as well, but they conclude that such an assumption is reasonable. From the spectroscopically derived parameters presented in Table 1, we do not expect any of our stars to be in this regime, and we will therefore treat radial velocity variations as attributed to binarity for the remainder of this paper.

For several targets, additional data is needed because the current variations are small, or rely heavily on the accuracy and comparison between literature data taken at different telescopes and analyzed by different teams. This is true for example for J1422+0031, for which the current binarity is based on three measurements and 53327-2044-515, that only shows clear evidence for binarity when our data set and the literature are combined. We continue to pursue follow-up observations, and anticipate to be able to constrain these particular cases better in future work.

3.2 Quantifying binarity

Following Lucatello et al. (2005), we first quantify our results by calculating the χ^2 value for the radial velocity distribution.

$$\chi^2 = \sum_{i=1}^{n} \left(\frac{v_{r_i} - \bar{v_r}}{\sigma_{v_{r_i}}} \right)^2 \quad (1)$$

We subsequently evaluate the probability that the radial velocities observed are compatible within the measurement errors expressed as $p(\chi^2|f)$, where f is the number of degrees of freedom. A small p-value thus indicates a low probability that the observed scatter in velocities is due to measurement errors, and points to an additional source of velocity variability. However, instead of a simple mean for all observations, we are using a mean value that is weighted by the observational errors. We find that the use of a weighted mean is critical for obtaining the correct χ^2 in datasets where the magnitude of the errors varies substantially from observation to observation for the same star (for instance, because different datasets are combined or exposure times vary). Therefore we use:

$$\bar{v_r} = \frac{\sum_{i=1}^{n} w_i v_{r_i}}{\sum_{i=1}^{n} w_i} \text{ and } w_i = \frac{1}{\sigma^2_{v_{r_i}}} \quad (2)$$

p-Values for our dataset, as well as for the literature and combined datasets, are given in Table 1. We note that Lucatello et al. (2005) include a multiplication by a factor 3 in all σ-values. This extra factor is motivated by the work of Preston & Sneden (2001) on multiple observations of giant stars, but is nevertheless quite arbitrary. In this work, we use the 1σ errors, except in the last column of the table, where we have included this extra factor of 3. From a comparison between the results with 1σ and 3σ errors, it is clear that the treatment of errors can be a driving parameter for the derivation of the binary fraction of the population.

3.3 Period analysis

A second step, after detecting variability, is to constrain the parameters of the stars' binary orbits, and thus gain a deeper physical insight in the possible pollution of these stars by companions. Shown in Figure 2 are periodograms for HE 1150-0428 and HE 1506-0113 from a period analysis of the (unevenly sampled) time series of radial velocity monitoring using Equation 1. from Horne & Baliunas (1986). This method is equivalent to a least square-fitting of sine curves to the data. The minimum period sampled is taken as the average sampling frequency for the five radial velocity datapoints closest in time (the minimum amount required to do a period analysis), the time between the first and last data point is the maximum period sampled. The peaks are checked against false positives by additionally performing the same analysis on a constant function with exact same sampling as the real data (see dotted lines in Fig-

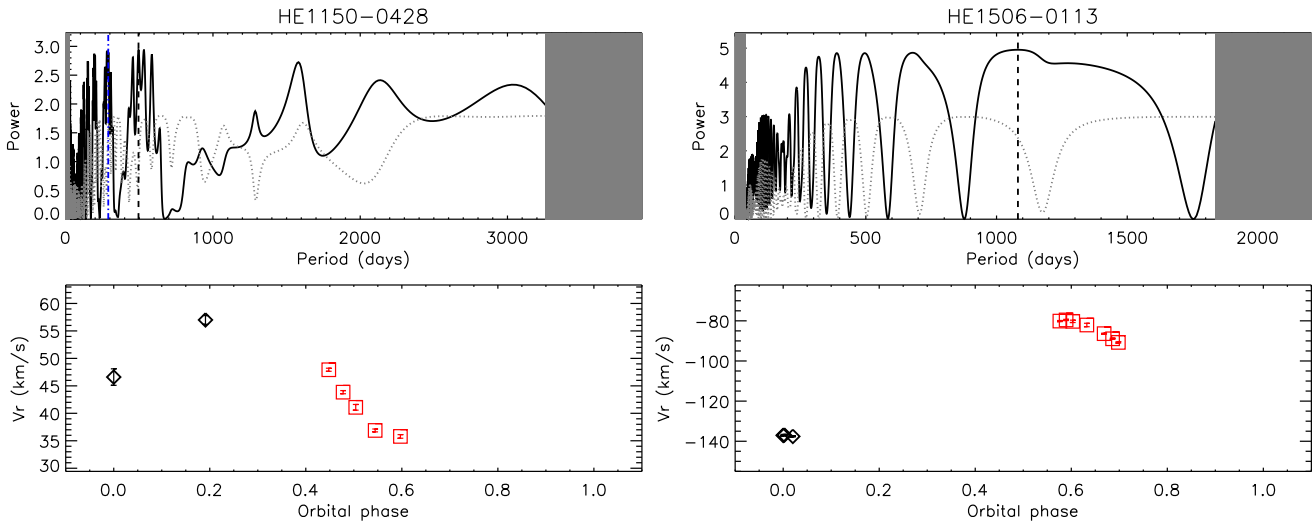

Figure 2. Periodograms of HE 1150-0428 and HE 1506-0113 based on all data, both literature and from this team (black diamonds and red squares in the bottom panel). The black line in the top panel indicates the power of the period solution. The same analysis is subsequently performed on a constant function with exact same sampling as the real data to check for any peaks that might be spurious results due to the sampling alone (dotted grey line). Various different periods are still very likely with the current data ranging from several weeks or months to years. The most likely orbital period from this analysis is highlighted by a dashed vertical black line. In the top left panel the blue dot-dashed line indicates a period of 289 days as found by Andersen et al., in preparation for the same star. Orbital phases for the velocity data for our most likely possibile orbit period are shown in the bottom panel.

ure 2); any peaks that correspond between the filled and dotted lines might be spurious results due to the sampling alone.

Various different periods, ranging from several weeks or months to years, are still very likely with the current data for both stars. More data with a good cadence will be required to more accurately define their periods. We note that Cohen et al. (2013) mention that a period of 289 days for HE 1150-0428 was found by Andersen et al., in preparation. Indeed, such a period would be consistent with our results, as highlighted by the blue vertical dot-dashed line in the bottom left panel of Figure 2.

4 CONSTRAINING BINARY FRACTION AND BINARY PERIODS FOR CARBON-ENHANCED METAL-POOR STARS

We use tailored Monte Carlo simulations combined with a maximum likelihood analysis to constrain the binary fraction and binary periods for various types of carbon-enhanced stars, and investigate their nature. The binary fraction and period are investigated simultaneously because they are degenerate. If only a relatively small number of stars shows radial velocity variations, this can point towards both a lower binary fraction or a higher average period; in the latter case the observational cadence – which is often on the order of years – might not be able to pick up any signal of variations with enough accuracy. To test both parameters, we draw 10,000 realizations of radial velocity datasets from a simulation with a certain combination of binary fraction (0 to 100%) and a cut-off period for these binaries. The mock datasets have the same cadence and are convolved with the same velocity errors as the observed datasets.

Parameters for the orbits of the binary stars are randomly assigned using constraints derived from the study of Duquennoy & Mayor (1991) in the Local Neighbourhood. We stress here that it is unclear if indeed our data will follow the same characteristics as the Solar Neighbourhood binaries, but – lacking any other constraints – it seems a reasonable assumption. We select stellar mass ratios for the binary pair from Duquennoy & Mayor (1991), but constrain the mass of the star observed $M_1 = 0.8\,\mathrm{M}_{\odot}$, consistent with an old age (sub)giant. A comparison of the stellar parameters in Table 1 confirms that this is indeed the expected mass for a large majority of the stars if they are of old age ($\sim$ 13 Gyr). Eccentricities are selected from a thermal distribution. The inclination i and the longitude at the ascending node ω are picked from a uniform distribution. The initial phase ν_0 is randomly selected from a distribution in accordance with the selected eccentricity of the orbit (i.e., uniformly for a circular orbit, but more likely to be at apocentre for an highly elliptical orbit).

The orbital periods for the binaries (if the binary fraction is not zero), P in days, are characterized following Duquennoy & Mayor (1991) by $\overline{\log P} = 4.8$ and $\sigma_{logP} = 2.3$. We introduce an upper and lower limit to the periods the mock stars are allowed to have. The applied lower limit excludes really short period binaries from our simulations; we set it at the 2σ level of $\sim$1 day and this is kept the same for all simulations. The upper limit is consequently varied as a second free parameter (besides the binary fraction), and ranges from almost a year up to the 2σ upper level for the Solar Neighbourhood distribution of $\sim$ 7 million years, in total covering six orders of magnitude.

We use a maximum likelihood analysis to return the most likely parameters characterizing the observed distribution. We compare the modeled distributions, M, to our datasets, D, by constructing histograms of the mutual independent velocity variations for each star, i and each observation t, using the first measured velocity as a reference point.

$$\Delta v_{i,t} = \frac{|v_{r_{i,0}} - v_{r_{i,t}}|}{(\sigma^2_{v_{r_{i,0}}} + \sigma^2_{v_{r_{i,t}}})^{\frac{1}{2}}} \qquad (3)$$

Figure 3 shows how the two parameters that we allow to vary – the binary fraction, f_{bin}, and maximum period, P_{max} – change

Star	HJD -2456000	v_r ($\mathrm{km\,s^{-1}}$)	σ_{vr_i} ($\mathrm{km\,s^{-1}}$)
53327-2044-515	487.93494	−199.12	1.39
53327-2044-515	510.87326	−205.21	2.60
53327-2044-515	522.84846	−198.70	4.39
BD +44-493	330.61789	−150.26	0.37
BD +44-493	339.62141	−150.08	0.37
BD +44-493	486.95551	−150.17	0.30
BD +44-493	508.91578	−149.94	0.32
BS 16929-005	341.81244	−50.62	0.26
BS 16929-005	366.74166	−50.61	0.77
BS 16929-005	396.88416	−50.48	0.29
BS 16929-005	469.68353	−50.44	0.95
BS 16929-005	479.65853	−50.18	0.26
CS 22878-027	384.87258	−91.41	0.36
CS 22878-027	389.85421	−91.99	0.53
CS 22878-027	420.76769	−91.14	0.57
CS 22878-027	455.68007	−91.16	0.26
CS 22878-027	480.77878	−91.64	0.66
CS 22878-027	507.70591	−91.76	0.29
CS 22949-037	485.92583	−126.00	0.36
CS 22949-037	506.86908	−125.84	0.27
CS 22957-027	487.95236	−60.79	0.53
CS 22957-027	505.94683	−60.75	0.41
CS 29502-092	458.95257	−66.93	0.40
CS 29502-092	478.90277	−66.72	0.35
CS 29502-092	506.89918	−66.73	0.54
HE 1150-0428	339.88474	47.93	0.28
HE 1150-0428	354.83867	43.85	0.29
HE 1150-0428	367.80309	41.09	0.52
HE 1150-0428	387.76986	36.88	0.26
HE 1150-0428	413.69469	35.79	0.33
HE 1300+0157	330.89601	74.86	0.37
HE 1300+0157	355.83157	74.29	0.55
HE 1300+0157	368.90131	74.42	0.45
HE 1300+0157	374.77741	73.60	0.84
HE 1300+0157	413.78680	75.19	0.48
HE 1300+0157	459.66750	74.39	0.29
HE 1506-0113	355.93837	−80.12	0.27
HE 1506-0113	369.89926	−79.55	0.29
HE 1506-0113	384.94103	−80.25	0.59
HE 1506-0113	416.85083	−82.07	0.86
HE 1506-0113	455.74001	−86.39	0.28
HE 1506-0113	474.67805	−88.93	0.29
HE 1506-0113	487.65958	−90.74	0.33
SDSS J1422+0031	442.65168	−124.63	0.50
SDSS J1613+5309	442.75102	0.07	0.26
SDSS J1613+5309	512.70831	−0.60	0.88
SDSS J1746+2455	442.74986	78.03	0.28
SDSS J1746+2455	455.70036	79.52	1.80
SDSS J1746+2455	487.82824	78.56	0.70
SDSS J2206-0925	481.91425	14.66	0.26
Segue 1-7	339.69733	204.01	1.70
Segue 1-7	367.61593	205.26	3.06
Segue 1-7	391.74756	205.04	0.27

Table 2. Data added in this program

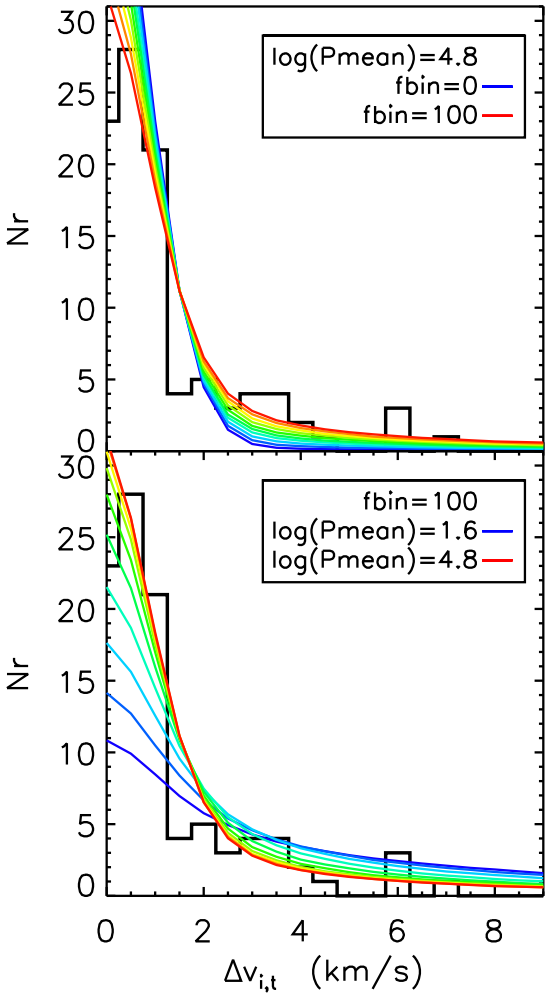

Figure 3. $\Delta v_{i,t}$ for the full CEMP-no dataset (literature + this work) overplotted with the normalized curve for 10,000 simulated realizations with similar cadence and errors. In the simulations the binary fraction and maximum period are left variable. The top panel shows how – at a Solar Neighbourhood value for P_{max} (and therefore P_{mean} = 4.8) – the distribution changes from no binaries (blue) to 100% (red). The bottom panel shows how – at a fixed binary fraction of 100% – the distribution changes from a value for P_{max} 2σ away from the solar mean ($10^{9.4}$ days, red) to our adopted smallest maximum value of 312 days (blue).

the distribution of 10,000 mock datasets in this space. Varying any of the two parameters will change the peak height and the tail of the distribution. It is clear that some degeneracy between the two parameters is met. Subsequently, we determine the most likely values for our variables by applying Bayes' theorem and assuming a uniform prior probability of the parameters. Assuming Poisson uncertainties in each separate histogram bin, we can express the relative posterior probability distribution for each combination of f_{bin} and P_{max} considered as

$$p(f_{bin}, P_{max}|D, M) \propto \prod_{b=1}^{N} \frac{m_b^{d_b} \mathrm{e}^{-m_b}}{d_b!}, \quad (4)$$

where d_b is the number of velocities measured with a certain variation in the dataset, and m_b the expected number of observa-

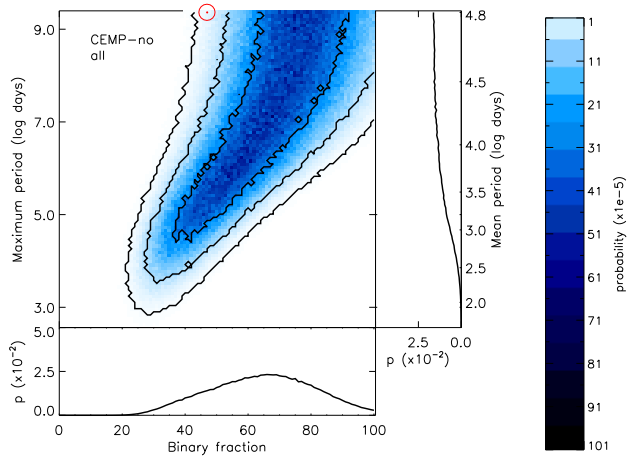

Figure 4. The relative posterior probability (see text for details) of each of the combinations of binary fraction and maximum period for the full sample of CEMP-no stars. Contour levels are drawn at the 1-, 2- and 3-σ levels. The probabilities marginalized over one of the free parameters are shown in an extra panel next to and below the contour level plots. The binarity fraction and period distribution in the Solar Neighbourhood among solar type stars is marked with a red solar symbol.

tions in that same velocity variation bin from the model, normalized to the same number of total observations as in the dataset. For practical reasons we approximate the Poisson distribution by a Gaussian distribution with mean m_b and variance m_b for values of m_b greater than 16. Each individual probability, $p(f_{bin}, P_{max}|D, M)$, is subsequently normalized by the sum of all probabilities across our model parameters.

As a simple test, we apply our method on the dataset of metal-poor stars by Carney et al. (2003). We find that an initial modeled binary fraction of 60% with a maximum period of log$P = 9.4$ (corresponding to the 2σ upper level, thus ensuring that the average period is identical to that derived by Duquennoy & Mayor 1991, in the Local Neighbourhood) convolved with the cadence and errors of their dataset returns 34% detectable binaries with $p(\chi^2|f) < 0.01$, in good accord with their findings in the data (32%).

4.1 A maximum likelihood analysis for the CEMP-no sample

To obtain a complete set of CEMP-no velocity monitoring, we combine all data presented in Table 1 with the stars published in Norris et al. (2013b), out of reach of HET, but for which multiple radial velocities are published (Aoki et al. 2004, 2006; Norris et al. 2007). For all literature data we exclude measurements that are published without an error, or do not mention the date of the observation.

Figure 4 shows the results of the posterior probability distribution as a function of the free parameters f_{bin} and P_{max}. As seen from this figure, a high amount of degeneracy is indeed met in constraining the binary fraction and the binary periods. The present data for the CEMP-no stars are only very marginally compatible with the Solar Neighbourhood binary properties among solar type stars (marked with a solar symbol in Figure 4, properties are taken from Duquennoy & Mayor (1991) and Raghavan et al. 2010).

In Figure 5 we split the sample of CEMP-no stars in the data from this work and the literature data. Although both subsamples show a similar trend in their 2-σ contours, it is interesting to see that the best solutions populate a different part of the diagram in both subsamples. Note that the probabilities indicate the best combination of both free parameters f_{bin} and P_{max} for the full dataset, and not a likelihood of the properties of any individual star. It is therefore not to be expected that a combination of the two panels of Figure 5 would result in Figure 4.

In the subset of data from this work only, it seems most likely that a few stars are in close period binaries, and the rest of the sample consists of single stars. In the literature dataset, the preferred solution points more toward a solution in which many stars are in binary systems, but many of these binary systems are wide binaries. As detailed above, these two solutions can be degenerate. One important consideration is that our cadence is too short to robustly detect long period binaries and therefore will likely classify long-period binaries as single stars. Another consideration that could drive the offset is the treatment of errors. If in the literature dataset systematic errors between the measurements are underestimated, for example, this will result in many (single) stars showing small variations that are not recognized as being caused by errors and will push the overall distribution towards more and wider binaries. A similar mismatch would occur if the literature errors are correct, but our errors are overestimated. With the current data in hand, it is difficult to fully break the degeneracy. It is however clear from both subsamples and the full dataset that there are clear binaries among these stars, that a Solar Neighbourhood distribution is only marginally acceptable, and that *if* all these stars are in binaries, most of these binaries will have to have very long periods.

4.2 The CEMP-s and CH-star samples

In Figure 6 we apply the same method to two other related samples of stars with extended radial velocity monitoring. First of all we take the CEMP-s sample from Lucatello et al. (2005), which consists of their data combined with radial velocity measurements from McClure & Woodsworth (1990); Norris, Ryan & Beers (1997a); Hill et al. (2000); Preston & Sneden (2000, 2001); Aoki et al. (2001, 2002a,b); Sneden, Preston & Cowan (2003); Van Eck et al. (2003); Lucatello et al. (2003); Cohen et al. (2003) and Barbuy et al. (2005). The number of observations and the length of the baselines for the CEMP-s velocity monitoring is fairly comparable to observational evidence of the CEMP-no stars, when the data in this work is added to the literature measurements.

Secondly, we have also analyzed the radial velocity monitoring for the much higher metallicity CH-, sgCH- and Ba II-stars as gathered by McClure & Woodsworth (1990) and McClure (1997a). These stars all show carbon and s-process enhancements, but they were originally placed in different classes based on their luminosity. For convenience, we will in the remainder of this paper refer to this combined sample as "CH-stars". We note that three stars in their sample were classified as CEMP-s stars by Lucatello et al. (2005) and are present in both samples. This fact illustrates the difficulty to draw sharp boundaries between various classes that are only loosely defined. A better physical understanding of their origin will help to define these classes in a more robust way.

Interestingly, the contours for both the CEMP-s and CH-stars are very well defined, both in binary fraction and in period. Our analysis shows with high probability that all, or almost all, CH-stars and CEMP-s stars are in binaries, confirming the conclusions of Lucatello et al. (2005) for CEMP-s stars and McClure, Fletcher & Nemec (1980); McClure (1983, 1984); Jorissen & Mayor (1988); McClure & Woodsworth (1990); McClure (1997a); Jorissen et al. (1998) for the CH-stars. In addi-

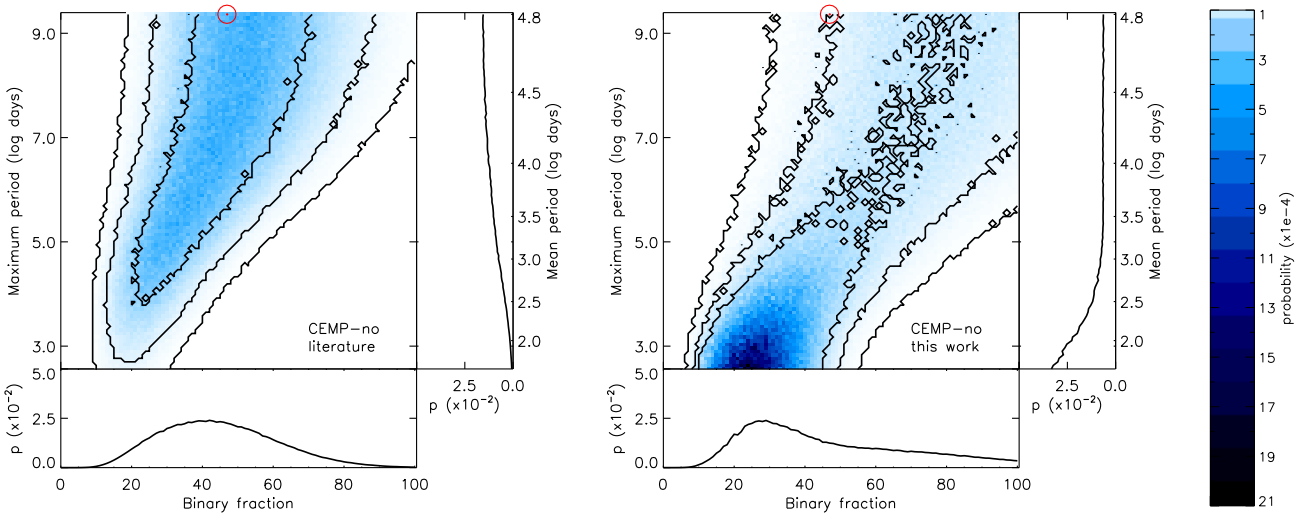

Figure 5. The relative posterior probability (see text for details) of each of the combinations of binary fraction and maximum period for the CEMP-no sample, divided into the data from this work and the data from literature. As in Figure 4, contour levels are drawn at the 1-, 2- and 3-σ levels, and the probabilities added over one of the free parameters are shown in an extra panel next to and below the contour level plots. The binarity fraction and period distribution in the Solar Neighbourhood among solar type stars is marked with a red solar symbol.

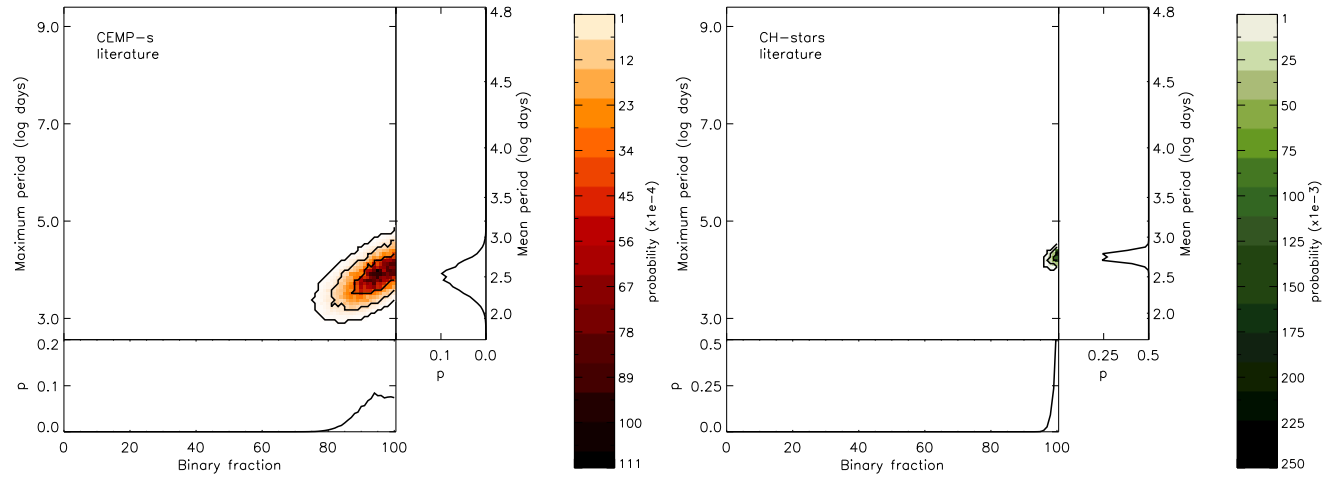

Figure 6. The relative posterior probability (see text for details) of each of the combinations of binary fraction and maximum period for the full literature samples of CEMP-s stars (Lucatello et al. 2005), and CH-stars (McClure & Woodsworth 1990; McClure 1997a). Contour levels are drawn at the 1-, 2- and 3-σ levels. The probabilities added over one of the free parameters are shown in an extra panel next to and below the contour level plots.

tion to these results in the literature, we also show convincingly that all these stars are in tighter binaries than the average Solar Neighbourhood binary system. Our most likely solution indicates in both cases a maximum period of ∼10,000-20,000 days, corresponding to an average period of ∼400-600 days.

Such relatively short periods are indeed expected in a scenario in which mass transfer is the mechanism responsible for their abnormal chemical pattern (e.g., Han et al. 1995). However, despite detailed modelling efforts, it is poorly understood what the driving mechanism for mass transfer onto companion stars would be. It has been argued that pure Roche-lobe overflow from an AGB star is usually unstable, and will lead to negligible accretion (Paczyński 1965; Ricker & Taam 2008). Therefore, much effort has been focussed on accretion by stellar winds, or a scenario called "wind Roche-lobe overflow (WRLOF)" (Mohamed & Podsiadlowski 2007; de Val-Borro, Karovska & Sasselov 2009; Abate et al. 2013). As shown in Abate et al. (2013), various unknowns in the exact parameters of the mass transfer will lead to different final orbits, due to angular momentum loss in the process. Our results for these stars seem in better qualitative agreement with their suite of models that include significant angular momentum loss. These models are characterized by a peak in the final periods somewhat higher than ∼1000 days. Instead, their standard wind models are peaked at periods significantly higher than our best-fit P_{max} (Izzard et al. 2009). However, we note that the shape of the period distribution in their models shows a double peak, whereas we still assume a lognormal distribution with a cutoff. We therefore caution against a

strict comparison of our derived maximum and mean to simulations and individual orbit solutions.

With this caveat in mind, our results – derived from the population as a whole – are also in qualitative agreement with the range of orbits found for several of these stars individually. Within the total sample of nineteen stars, the ten CEMP-s stars with orbital solutions have periods ranging from 3.4 to 4130 days, with an average period of 1200 days (Lucatello et al. 2005, and references therein). For the 32 stars monitored by McClure & Woodsworth (1990), 24 stars have orbital solution and show a range of periods from 80 to 4390 days and an average of 1650 days. Additionally, Jorissen et al. (1998) present a comparison of orbital solutions from radial velocity monitoring results (see also Udry et al. 1998a,b) of 93 binaries with (mild and strong) barium stars and stars classified as Tc-poor S stars - believed to be the cool descendants of barium stars. They find that the binary fraction, period distribution and eccentricities for all these classes differ from the typical orbital elements found among red giants in open clusters (Mermilliod 1996; Mermilliod et al. 2007, for an updated sample) in that they have a lower maximum eccentricity at a given period, which might be a sign of mass transfer. On the other hand, the orbital properties of the various barium and Tc-poor S star subsamples discussed in Jorissen et al. (1998) are similar to those found by McClure & Woodsworth (1990) and to each other.

While it has been hypothesized before that also CEMP-s and CH-stars as a class show a common origin, the excellent agreement in their binary properties shown here in this work puts this hypothesis on a much firmer footing.

4.3 All datasets compared

Another key result from the analysis presented above is that, with very high significance, the binary properties of the CEMP-s and CH-stars, as a population, do not overlap with that of the CEMP-no stars; as can be clearly seen when one compares Figure 4 with Figure 6.

Figure 7 shows the histograms of $\Delta v_{i,t}$ for the CEMP-s, CH-stars, all CEMP-no and the CEMP-no stars in this work with overplotted their best solution according to the Bayesian posterior probability detailed above. These figures highlight again the differences in the distributions between these datasets in a more direct way, most particularly between the measurements of the CEMP-s and CH-stars on the one hand and the CEMP-no samples on the other.

5 DISCUSSION:WHAT ARE THE CEMP-NO STARS?

In this section we will further investigate the remaining possible scenarios for the origin of the peculiar chemical composition of the CEMP-no population.

They are born with it.

The fact that some of the CEMP-no stars are in binaries does not automatically imply that mass transfer has to have happened. Perhaps the secondary has not evolved through an AGB phase, or mass transfer has not been effective. If we assume a similar distribution of periods, eccentricities etc., then – according to the observational evidence as presented in Figure 4 – a somewhat higher binary fraction than in the Solar Neighbourhood is favoured. This would be in agreement with claims that binarity is generally higher in lower metallicity populations (e.g. Carney et al. 2003). So one could argue that the binarity of these stars are as expected from star formation processes in "normal" populations, and need not be connected to their peculiar chemical properties. Several scenarios in the literature have been suggested in which these stars form out of a birth cloud enhanced with carbon-enhanced material and deficient in s-process material. We refer the reader to Norris et al. (2013b), Karlsson, Bromm & Bland-Hawthorn (2013) and Nomoto, Kobayashi & Tominaga (2013) for a detailed description of proposed scenarios and their (sometimes subtle) differences. Here, we instead highlight two main ideas. First, various models argue that the region could be enriched in C-rich material by the supernova and/or wind ejecta of Pop III stars where rotation of these stars plays a major role (e.g., Fryer, Woosley & Heger 2001; Meynet, Ekström & Maeder 2006; Chiappini et al. 2006; Karlsson 2006; Hirschi 2007; Chiappini et al. 2008; Meynet et al. 2010; Maeder & Meynet 2012; Cescutti et al. 2013). A second possibility involves a pristine gas cloud enriched by preceding supernovae explosions of more massive stars with fall-back, thereby locking in most heavy elements and expelling mainly lighter elements (Umeda & Nomoto 2003; Limongi, Chieffi & Bonifacio 2003; Iwamoto et al. 2005; Umeda & Nomoto 2005; Tominaga, Umeda & Nomoto 2007). As presented in Ito et al. (2013), the detailed abundance pattern of the brightest CEMP-no star, BD +44-493, seems to be consistent with this scenario and not with pollution from an AGB companion or by massive, fast-rotating stars.

As discussed by Bromm & Loeb (2003) once an enhancement in carbon and other light elements exists in a very metal-poor environment, this will aid the star formation process by shortening the timescale for cooling significantly (see also Frebel, Johnson & Bromm 2007b; Gilmore et al. 2013). The binary properties for CEMP-no stars are, in each of these scenarios, unrelated to their chemical history. We note that one prediction of this scenario is that should one be able to find and measure the properties of the binary companion; it will have a similar chemical composition as it most probably originated in the same birth cloud. Either of these scenarios suggest that the formation of CEMP-no stars is related to higher mass progenitors than of CEMP-s stars. As remarked by Carollo et al. (2014) and Lee et al. (2013b), studying the CEMP-no to CEMP-s ratio in various Galactic populations could therefore provide interesting clues about their Intitial Mass Function. On the other hand, differences in CEMP-no to CEMP-s stars in various populations could also be related to differences in binary fraction or properties, as we show in this work.

They are polluted.

From our analysis we find there is certainly some binarity present in the CEMP-no sample. Moreover, based on all radial velocity data currently in hand, we can not rule out that all CEMP-no stars are in binaries. However, if they are, many of these binary systems will have to be very wide. This questions the possibility of a scenario which involves mass transfer. We have convincingly shown that the binary population of CEMP-no stars is very different to that of the well-known classes of mass transfer binaries as CEMP-s and CH-stars. So, if CEMP-no stars would obtain their carbon excess from a companion, one would be tempted to look for a different transfer mechanism that would be able to act over a wider range of separations. As detailed in the previous section, it is somewhat debated if the mass transfer happens through Roche-lobe overflow, wind accretion or a combination. Each of the mechanisms proposed

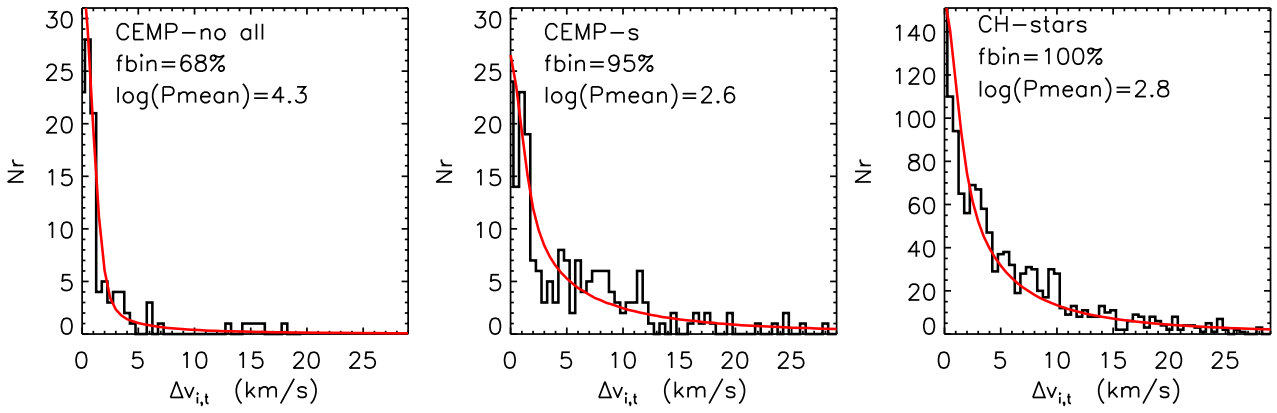

Figure 7. Histograms of each of distributions in $\Delta v_{i,t}$ for the CEMP-no measurements from this work and combined and from the literature samples of CEMP-s, CH-stars, with overplotted the most probable distributions from the simulations. The best-fitting parameters for the binary fraction and mean period are labelled in the panels.

would have a typical range of separations, and therefore periods, over which it would be most effective.

Additionally, we note that pollution processes do not necessarily involve binarity. Various of the pollution scenarios for the star's birth cloud as mentioned in the previous paragraph could also possibly pollute a star's atmosphere later on. One interesting candidate for such enrichment might be again massive stars going through a Wolf-Rayet (hereafter WR) phase, especially the sub-class of WR carbon stars. While individual WR stars enrich only small local bubbles < 10 pc in size (e.g., WR16, Duronea, Arnal & Bronfman 2013), WR stars within star forming regions can contribute to much larger bubbles. The star forming region LMC N51D (or DEML192, Davies, Elliott & Meaburn 1976) contains UV-bright O-stars and a WC5 star (Oey & Smedley 1998), and produces a wind-blown super-bubble 120 pc in size traced by several indicators including Hα and [S II] HST imaging (Chen et al. 2000), XMM-Newton X-ray imaging (Bomans et al. 2003), and Spitzer IRAC imaging (Chu et al. 2005). Starburst galaxies with many concentrated WR stars can show enrichments over even larger (kpc) scales. For instance, HST imaging of NGC 5253 by Calzetti et al. (2004) find S[II] filaments > 1 kpc from the ionizing starburst at the centre. While the C-enrichment and stellar wind strengths of WR stars are found to be metallicity dependent (e.g., Portinari, Chiosi & Bressan 1998; Maeder & Meynet 2012), the yields and stellar wind properties of massive rotating stars are predicted to be effective at all metallicities. Thus, whether from WR stars themselves or from the cumulative effects of the stellar winds from massive stars (especially massive rotating stars), it appears that carbon enrichments without neutron-capture elements could occur over large scales in star forming regions over a range of metallicities.

During their evolution they accreted dust-depleted gas.

Another mechanism that could lead to a carbon enhancement without neutron-capture elements would be the separation of gas and dust beyond the stellar surface, e.g., the formation of a debris disk, followed by the accretion of dust-depleted gas. Venn & Lambert (2008) compared the chemical abundances of two of the metal-poor C-rich stars to those of the chemically peculiar post-AGB, RV Tau, and Lambda Boo stars. There are some similarities that correlate with dust condensation temperature, and could imply that grain formation contributes to the chemical abundance pattern, rather than variations being due to natal or binary characteristics. However, one critical test of this hypothesis is in the abundance of sulphur and/or zinc, which have been found to be enriched in the chemically peculiar stars, or more accurately, they have not been depleted onto dust grains due to their low condensation temperatures. Unfortunately, the upper limits on sulphur and zinc in most of the metal-poor C-rich stars are insufficient to test this hypothesis; only one star, CS 22949-037 ([Fe/H] = -4.0), has upper limits on these two elements that are 1.5 dex below the expected values (Spite et al. 2011). For this star, its metal-poor and C-rich nature cannot be explained by the separation of dust and gas in the stellar envelop. Also, [Zn/Fe] is low in BD +44-493 (Ito et al. 2013) suggesting that it has not seen dust formation either. A second critical test of this hypothesis is the presence of infrared or sub-mm emission from the dust grains. Spectral energy distribution fitting for several ultra metal-poor CEMP-no stars show no excess emission below 22 microns (Venn et al. 2014, in preparation), consistent with a lack of circumstellar material. These observations cannot rule out cooler debris disks though, such as those found around close-in A-stars and Lambda Bootis stars (e.g., see Wyatt 2008; Booth et al. 2013). In conclusion, the separation of dust and gas in a cool debris disk is a valid hypothesis still for some - but definitely not all - CEMP-no stars.

They are the low-metallicity counterparts of R-stars.

As the CH-, sgCH- and Ba II-stars are the higher metallicity counterparts of CEMP-s (and possibly CEMP-r/s) stars, can we point out a high-metallicity equivalent for CEMP-no stars? Such a connection could help us to understand their formation mechanism. As proposed also by Cohen et al. (2006, 2013), the intriguing class of R-stars comes to mind (the "R"-classification hereby refers back to the R, N system of Cannon & Pickering (1918) and should not be confused with stars rich in r-process material). As described in Dominy (1984), these stars show carbon enhancements, but no s-process enhancements. Additionally and curiously, they show no signs *at all* of binarity at a very high significance level (McClure 1997b). As also shown in this work, the binary fraction among CEMP-no is most certainly not zero, as for the R-stars. The absence of binarity among R-stars led McClure (1997b) to argue that perhaps their absolute absence of binarity – much unlike any other population of stars we know – is a clue to their formation history.

He proposed these stars might have been in very close binaries and that a merging event between the companions might have led the carbon produced in the helium-core to be mixed outward. A subsequent prediction from this scenario is that there will be no sub-giant or dwarf R-stars (as they will have to be producing carbon in order for it to be available for mixing). This prediction seems to hold. This again implies that there is no connection between R-stars and CEMP-no stars. Unlike the R-stars, CEMP-no stars seem to be distributed over much of the HR-diagram, including the main-sequence and sub-giant branch.

They are a mixed bag.

The definition of the class of CEMP-no stars by Beers & Christlieb (2005) is mainly motivated by observational evidence, and might actually harbour stars from a variety of formation mechanisms that share a common carbon excess – and a common barium depletion ([Ba/Fe]$<$0). As noted before, a star can belong to multiple classes depending on its ratio of abundances in Ba, Eu and Fe. The possibility of a combination of formation mechanisms in the CEMP-no class is intriguing when looking at the data set from this work (right panel of Figure 5). Here we identify some stars clearly as short-period binaries, while the other stars are consistent with being single. We have searched the spectra of our close binary stars HE 1150-0428 and HE 1506-0113 for any sign of double lines, but did not find any signatures, most likely indicating that their companion is fainter (which would be expected if the companion went through an AGB phase already and is now a white dwarf). Could it be that in our CEMP-no class, truly second-generation stars (born with a peculiar chemistry that includes high carbon-enhancement) are mixed with stars that obtained their carbon enhancements later in their lives, by a mass-transferring binary or other mechanisms? As discussed before, mass-transfer mechanisms that would transfer carbon – but no or few s-process elements – are found in several model predictions for rotating or massive AGB stars (Herwig, Langer & Lugaro 2003; Herwig 2004; Siess, Goriely & Langer 2004), or AGB-stars with very high neutron-to-Fe-peak-element seed ratios (Busso, Gallino & Wasserburg 1999; Cohen et al. 2006).

It is worth pointing out here that the various stars in this CEMP-no sample, even though they are all enhanced in carbon and depleted in [Ba/Fe], do not show a similar chemical pattern for other elements. This might superficially be taken as an indication for a variety of origins among these stars. Most theoretical models describing the origin of these stars focus on the explanation of the abundance pattern of one of the four hyper-metal-poor stars ([Fe/H]< -5), and do not simultaneously explain the full sample as researched here (but see Tominaga, Iwamoto & Nomoto 2013, who provide an individual best-fit Pop III SN model for 48 extremely metal-poor stars).

However, continuing the thought that there exist different formation mechanisms into one class, it must be remarked that we also see no striking similarities in the patterns of those that appear to be in close binaries. For instance, the two stars with outstanding radial velocity variations, HE 1150-0428 and HE 1506-0113, show very different abundance patterns, even though they have very similar metallicities and comparable temperatures and gravities (Yong et al. 2013a; Cohen et al. 2006). HE 1506-0113 is only moderately enhanced in [N/Fe], and shows significant enhancements in Na and Mg. On the other hand, HE 1150-0428 shows a higher [C/Fe] and very high enhancement in [N/Fe], solar-like [Na/Fe], but enhancements in [Ti/Fe] and in particular [Ca/Fe] (see also Figure 7. of Norris et al. 2013b, for a direct comparison). Both stars are depleted in [Sr/Fe], but HE 1150-0428 much less so. Unfortunately, neither of the two stars has a robustly measured [Eu/Fe] abundance, making it difficult to comment on the possibility that these might also be of the CEMP-r or CEMP-r/s class. With the (lack of) present evidence it is very well possible that the CEMP-no class of stars includes any combination of the above mentioned formation scenarios. Among other avenues, we expect further insight in these mysterious stars to be obtained in the coming years by a careful analysis of their abundance patterns, focussing on the abundances of light elements as well as their neutron-capture elements (see for instance the work of Masseron et al. 2012; Norris et al. 2013b; Ito et al. 2013; Hansen et al. 2014; Keller et al. 2014, emphasizing the importance of the lighter elements).

6 CONCLUSIONS: THE RELATIONSHIP BETWEEN THE VARIOUS CLASSES OF CARBON-STARS

In this work we have investigated the binary properties of three subclasses of carbon enhanced stars for which radial velocity monitoring is available: The CEMP-s stars that are metal-poor and show enhancements in carbon and barium; the combined group of CH-stars (consisting of (sg)CH- and Ba II - stars) that share these abundance signatures at higher metallicities; and the CEMP-no stars, metal-poor stars with enhancements in carbon but not in barium. For the latter group we have presented new radial velocity monitoring from the HET, thereby greatly improving the available information on these mysterious stars. With this new data two CEMP-no stars show clear variabilities in their radial velocities, indicating they are part of binary system. For various other stars more data is needed.

From a comparison of the data available for each of these subgroups with simulations in which the binary fraction and maximum period from the period distribution is treated as a free parameter, we can draw the following conclusions:

- Binary properties in CEMP-no stars are marginally consistent with the observed Solar Neighbourhood binary fraction and periods.
- *If* CEMP-no stars are all in binaries, some of them have very long periods. A solution in which the binary fraction is lower, but the binaries have shorter periods, is also very likely.
- Binarity of CEMP-s stars is well-modeled with an (almost) 100% binary fraction and a maximum period $\sim$20,000 days.
- CEMP-s stars and CH-stars share similar binary properties. This places the hypothesis that CEMP-s stars are the lower metallicity equivalents of the CH-stars on a much firmer footing.
- CEMP-no and CEMP-s stars have very different binary properties, therefore it is unlikely their overabundance in carbon is obtained via the same physical mechanism.
- The CEMP-no population are not the metal-poor equivalents of R-stars. A primary origin for the carbon enhancement remains very likely, although an origin from a binary companion using a mechanism that can operate for long period systems and which does not transfer s-process elements can not yet be ruled out. Another distinct possibility is that the CEMP-no class contains various physical sub-classes in itself.

ACKNOWLEDGMENTS

We thank Falk Herwig and David Hartwick for very helpful discussions and the referee for insightful suggestions that helped to improve the manuscript. The authors are indebted to the International Space Science Institute (ISSI), Bern, Switzerland, for supporting and funding the international team "First stars in dwarf galaxies". E.S. also gratefully acknowledges the Canadian Institute for Advanced Research (CIFAR) Global Scholar Academy and the Canadian Institute for Theoretical Astrophysics (CITA) National Fellowship for partial support. The Hobby-Eberly Telescope (HET) is a joint project of the University of Texas at Austin, the Pennsylvania State University, Stanford University, Ludwig-Maximilians-Universität München, and Georg-August-Universität Göttingen. The HET is named in honor of its principal benefactors, William P. Hobby and Robert E. Eberly.

REFERENCES

Abate C., Pols O. R., Izzard R. G., Mohamed S. S., de Mink S. E., 2013, A&A, 552, A26
Allen D. M., Ryan S. G., Rossi S., Beers T. C., Tsangarides S. A., 2012, A&A, 548, A34
Aoki W., Beers T. C., Christlieb N., Norris J. E., Ryan S. G., Tsangarides S., 2007, ApJ, 655, 492
Aoki W. et al., 2013, AJ, 145, 13
—, 2006, ApJ, 639, 897
Aoki W., Norris J. E., Ryan S. G., Beers T. C., Ando H., 2002a, ApJ, 576, L141
—, 2002b, PASJ, 54, 933
Aoki W., Norris J. E., Ryan S. G., Beers T. C., Christlieb N., Tsangarides S., Ando H., 2004, ApJ, 608, 971
Aoki W. et al., 2001, ApJ, 561, 346
Barbuy B., Spite M., Spite F., Hill V., Cayrel R., Plez B., Petitjean P., 2005, A&A, 429, 1031
Barklem P. S. et al., 2005, A&A, 439, 129
Beers T. C., Christlieb N., 2005, ARA&A, 43, 531
Bisterzo S., Gallino R., Straniero O., Cristallo S., Käppeler F., 2012, MNRAS, 422, 849
Bomans D. J., Rossa J., Weis K., Dennerl K., 2003, in IAU Symposium, Vol. 212, A Massive Star Odyssey: From Main Sequence to Supernova, van der Hucht K., Herrero A., Esteban C., eds., p. 637
Booth M. et al., 2013, MNRAS, 428, 1263
Bromm V., Loeb A., 2003, Nature, 425, 812
Busso M., Gallino R., Wasserburg G. J., 1999, ARA&A, 37, 239
Caffau E. et al., 2011, Nature, 477, 67
Calzetti D., Harris J., Gallagher, III J. S., Smith D. A., Conselice C. J., Homeier N., Kewley L., 2004, AJ, 127, 1405
Cannon A. J., Pickering E. C., 1918, Annals of Harvard College Observatory, 91, 1
Carney B. W., Latham D. W., Stefanik R. P., Laird J. B., 2008, AJ, 135, 196
Carney B. W., Latham D. W., Stefanik R. P., Laird J. B., Morse J. A., 2003, AJ, 125, 293
Carollo D. et al., 2012, ApJ, 744, 195
Carollo D., Freeman K., Beers T., Placco V., Tumlinson J., Martell S., 2014, ApJ, submitted, (arXiv:1401.0574)
Cayrel R. et al., 2004, A&A, 416, 1117
Cescutti G., Chiappini C., Hirschi R., Meynet G., Frischknecht U., 2013, A&A, 553, A51
Chen C.-H. R., Chu Y.-H., Gruendl R. A., Points S. D., 2000, AJ, 119, 1317
Chiappini C., Ekström S., Meynet G., Hirschi R., Maeder A., Charbonnel C., 2008, A&A, 479, L9
Chiappini C., Hirschi R., Meynet G., Ekström S., Maeder A., Matteucci F., 2006, A&A, 449, L27
Christlieb N., 2003, in Reviews in Modern Astronomy, Vol. 16, Reviews in Modern Astronomy, R. E. Schielicke, ed., p. 191
Christlieb N., Gustafsson B., Korn A. J., Barklem P. S., Beers T. C., Bessell M. S., Karlsson T., Mizuno-Wiedner M., 2004, ApJ, 603, 708
Chu Y.-H. et al., 2005, ApJ, 634, L189
Cohen J. G., Christlieb N., McWilliam A., Shectman S., Thompson I., Melendez J., Wisotzki L., Reimers D., 2008, ApJ, 672, 320
Cohen J. G., Christlieb N., Qian Y.-Z., Wasserburg G. J., 2003, ApJ, 588, 1082
Cohen J. G., Christlieb N., Thompson I., McWilliam A., Shectman S., Reimers D., Wisotzki L., Kirby E., 2013, ApJ, 778, 56
Cohen J. G. et al., 2006, AJ, 132, 137
—, 2005, ApJ, 633, L109
Davies R. D., Elliott K. H., Meaburn J., 1976, Memoirs of the RAS, 81, 89
de Val-Borro M., Karovska M., Sasselov D., 2009, ApJ, 700, 1148
Depagne E. et al., 2002, A&A, 390, 187
Dominy J. F., 1984, ApJS, 55, 27
Duquennoy A., Mayor M., 1991, A&A, 248, 485
Duronea N. U., Arnal E. M., Bronfman L., 2013, A&A, 551, A71
François P. et al., 2007, A&A, 476, 935
Frebel A. et al., 2005, Nature, 434, 871
—, 2006, ApJ, 652, 1585
Frebel A., Johnson J. L., Bromm V., 2007b, MNRAS, 380, L40
Frebel A., Norris J. E., Aoki W., Honda S., Bessell M. S., Takada-Hidai M., Beers T. C., Christlieb N., 2007a, ApJ, 658, 534
Fryer C. L., Woosley S. E., Heger A., 2001, ApJ, 550, 372
Gilmore G., Norris J. E., Monaco L., Yong D., Wyse R. F. G., Geisler D., 2013, ApJ, 763, 61
Gunn J. E., Griffin R. F., 1979, AJ, 84, 752
Han Z., Eggleton P. P., Podsiadlowski P., Tout C. A., 1995, MNRAS, 277, 1443
Hansen T., Andersen J., Nordström B., Buchhave L. A., Beers T. C., 2011, ApJ, 743, L1
Hansen T., Andersen J., Nordtröm B., 2013, arXiv:1301.7208
Hansen T. et al., 2014, A&A, submitted
Herwig F., 2004, ApJ, 605, 425
Herwig F., Langer N., Lugaro M., 2003, ApJ, 593, 1056
Hill V. et al., 2000, A&A, 353, 557
Hirschi R., 2007, A&A, 461, 571
Honda S., Aoki W., Kajino T., Ando H., Beers T. C., Izumiura H., Sadakane K., Takada-Hidai M., 2004, ApJ, 607, 474
Horne J. H., Baliunas S. L., 1986, ApJ, 302, 757
Ito H., Aoki W., Beers T. C., Tominaga N., Honda S., Carollo D., 2013, ApJ, 773, 33
Ito H., Aoki W., Honda S., Beers T. C., 2009, ApJ, 698, L37
Iwamoto N., Umeda H., Tominaga N., Nomoto K., Maeda K., 2005, Science, 309, 451
Izzard R. G., Glebbeek E., Stancliffe R. J., Pols O. R., 2009, A&A, 508, 1359
Jorissen A., Mayor M., 1988, A&A, 198, 187
Jorissen A., Van Eck S., Mayor M., Udry S., 1998, A&A, 332, 877
Karlsson T., 2006, ApJ, 641, L41

Karlsson T., Bromm V., Bland-Hawthorn J., 2013, Reviews of Modern Physics, 85, 809
Keller S. C. et al., 2014, Nature, in press (arXiv:1402.1517)
Komiya Y., Suda T., Minaguchi H., Shigeyama T., Aoki W., Fujimoto M. Y., 2007, ApJ, 658, 367
Lai D. K., Bolte M., Johnson J. A., Lucatello S., Heger A., Woosley S. E., 2008, ApJ, 681, 1524
Lee Y. S. et al., 2013, AJ, 146, 132
Lee Y. S., Suda T., Beers T. C., Lucatello S., 2013b, ApJ, submitted (arXiv:1310.3277)
Limongi M., Chieffi A., Bonifacio P., 2003, ApJ, 594, L123
Lucatello S., Beers T. C., Christlieb N., Barklem P. S., Rossi S., Marsteller B., Sivarani T., Lee Y. S., 2006, ApJ, 652, L37
Lucatello S., Gratton R., Cohen J. G., Beers T. C., Christlieb N., Carretta E., Ramírez S., 2003, AJ, 125, 875
Lucatello S., Tsangarides S., Beers T. C., Carretta E., Gratton R. G., Ryan S. G., 2005, ApJ, 625, 825
Lugaro M., Karakas A. I., Stancliffe R. J., Rijs C., 2012, ApJ, 747, 2
Maeder A., Meynet G., 2012, Reviews of Modern Physics, 84, 25
Marsteller B., Beers T. C., Rossi S., Christlieb N., Bessell M., Rhee J., 2005, Nuclear Physics A, 758, 312
Masseron T., Johnson J. A., Lucatello S., Karakas A., Plez B., Beers T. C., Christlieb N., 2012, ApJ, 751, 14
Masseron T., Johnson J. A., Plez B., van Eck S., Primas F., Goriely S., Jorissen A., 2010, A&A, 509, A93
McClure R. D., 1983, ApJ, 268, 264
—, 1984, ApJ, 280, L31
—, 1997a, PASP, 109, 536
—, 1997b, PASP, 109, 256
McClure R. D., Fletcher J. M., Nemec J. M., 1980, ApJ, 238, L35
McClure R. D., Woodsworth A. W., 1990, ApJ, 352, 709
McWilliam A., Preston G. W., Sneden C., Searle L., 1995b, AJ, 109, 2757
McWilliam A., Preston G. W., Sneden C., Shectman S., 1995a, AJ, 109, 2736
Mermilliod J.-C., 1996, in Astronomical Society of the Pacific Conference Series, Vol. 90, The Origins, Evolution, and Destinies of Binary Stars in Clusters, Milone E. F., Mermilliod J.-C., eds., p. 475
Mermilliod J.-C., Andersen J., Latham D. W., Mayor M., 2007, A&A, 473, 829
Meynet G., Ekström S., Maeder A., 2006, A&A, 447, 623
Meynet G., Hirschi R., Ekstrom S., Maeder A., Georgy C., Eggenberger P., Chiappini C., 2010, A&A, 521, A30
Mohamed S., Podsiadlowski P., 2007, in Astronomical Society of the Pacific Conference Series, Vol. 372, 15th European Workshop on White Dwarfs, Napiwotzki R., Burleigh M. R., eds., p. 397
Nomoto K., Kobayashi C., Tominaga N., 2013, ARA&A, 51, 457
Norris J. E. et al., 2013a, ApJ, 762, 25
Norris J. E., Christlieb N., Korn A. J., Eriksson K., Bessell M. S., Beers T. C., Wisotzki L., Reimers D., 2007, ApJ, 670, 774
Norris J. E., Gilmore G., Wyse R. F. G., Yong D., Frebel A., 2010, ApJ, 722, L104
Norris J. E., Ryan S. G., Beers T. C., 1997a, ApJ, 488, 350
—, 1997b, ApJ, 489, L169
—, 2001, ApJ, 561, 1034
Norris J. E. et al., 2013b, ApJ, 762, 28
Oey M. S., Smedley S. A., 1998, AJ, 116, 1263
Paczyński B., 1965, Acta Astron., 15, 89
Piersanti L., Cristallo S., Straniero O., 2013, ApJ, 774, 98
Placco V. M., Frebel A., Beers T. C., Christlieb N., Lee Y. S., Kennedy C. R., Rossi S., Santucci R. M., 2014, ApJ, 781, 40
Portinari L., Chiosi C., Bressan A., 1998, A&A, 334, 505
Preston G. W., Sneden C., 2000, AJ, 120, 1014
—, 2001, AJ, 122, 1545
Raghavan D. et al., 2010, ApJS, 190, 1
Ramsey L. W. et al., 1998, in Society of Photo-Optical Instrumentation Engineers (SPIE) Conference Series, Vol. 3352, Advanced Technology Optical/IR Telescopes VI, Stepp L. M., ed., pp. 34–42
Ricker P. M., Taam R. E., 2008, ApJ, 672, L41
Rossi S., Beers T. C., Sneden C., 1999, in Astronomical Society of the Pacific Conference Series, Vol. 165, The Third Stromlo Symposium: The Galactic Halo, B. K. Gibson, R. S. Axelrod, & M. E. Putman, ed., p. 264
Ryan S. G., Aoki W., Norris J. E., Beers T. C., 2005, ApJ, 635, 349
Setiawan J., Pasquini L., da Silva L., von der Lühe O., Hatzes A., 2003, A&A, 397, 1151
Shetrone M. et al., 2007, PASP, 119, 556
Siess L., Goriely S., Langer N., 2004, A&A, 415, 1089
Sneden C., Preston G. W., Cowan J. J., 2003, ApJ, 592, 504
Spite M. et al., 2011, A&A, 528, A9
Spite M., Caffau E., Bonifacio P., Spite F., Ludwig H.-G., Plez B., Christlieb N., 2013, A&A, 552, A107
Spite M. et al., 2005, A&A, 430, 655
Suda T., Aikawa M., Machida M. N., Fujimoto M. Y., Iben, Jr. I., 2004, ApJ, 611, 476
Tominaga N., Iwamoto N., Nomoto K., 2013, ApJ, accepted (arXiv:1309.6734)
Tominaga N., Umeda H., Nomoto K., 2007, ApJ, 660, 516
Tull R. G., 1998, in Society of Photo-Optical Instrumentation Engineers (SPIE) Conference Series, Vol. 3355, Optical Astronomical Instrumentation, D'Odorico S., ed., pp. 387–398
Udry S., Jorissen A., Mayor M., Van Eck S., 1998a, A&AS, 131, 25
Udry S., Mayor M., Van Eck S., Jorissen A., Prevot L., Grenier S., Lindgren H., 1998b, A&AS, 131, 43
Umeda H., Nomoto K., 2003, Nature, 422, 871
—, 2005, ApJ, 619, 427
Van Eck S., Goriely S., Jorissen A., Plez B., 2003, A&A, 404, 291
Venn K. A., Lambert D. L., 2008, ApJ, 677, 572
Wright J. T., 2005, PASP, 117, 657
Wyatt M. C., 2008, ARA&A, 46, 339
Yong D. et al., 2013a, ApJ, 762, 26
—, 2013b, ApJ, 762, 27